

# The Critical Hopping Parameter in $\mathcal{O}(a)$ improved Lattice QCD

H. Panagopoulos and Y. Proestos\*

*Department of Physics, University of Cyprus, P.O. Box 20537, Nicosia CY-1678, Cyprus*

*email: [haris@ucy.ac.cy](mailto:haris@ucy.ac.cy), [yiannis@mps.ohio-state.edu](mailto:yiannis@mps.ohio-state.edu)*

(October 29, 2018)

## Abstract

We calculate the critical value of the hopping parameter,  $\kappa_c$ , in  $\mathcal{O}(a)$  improved Lattice QCD, to two loops in perturbation theory. We employ the Sheikholeslami-Wohlert (clover) improved action for Wilson fermions.

The quantity which we study is a typical case of a vacuum expectation value resulting in an additive renormalization; as such, it is characterized by a power (linear) divergence in the lattice spacing, and its calculation lies at the limits of applicability of perturbation theory.

The dependence of our results on the number of colors  $N$ , the number of fermionic flavors  $N_f$ , and the clover parameter  $c_{\text{SW}}$ , is shown explicitly. We compare our results to non perturbative evaluations of  $\kappa_c$  coming from Monte Carlo simulations.

**Keywords:** Lattice QCD, Lattice perturbation theory, Hopping parameter, Clover action.

**PACS numbers:** 11.15.-q, 11.15.Ha, 12.38.G.

---

\*Present address: Department of Physics, Ohio State University, Columbus, OH 43210, USA

## I. INTRODUCTION

In this paper we calculate the critical value of the hopping parameter  $\kappa_c$  in Lattice QCD, to two loops in perturbation theory. We employ the  $\mathcal{O}(a)$  improved Sheikholeslami-Wohlert [1] (clover) action for Wilson fermions; this action is widely used nowadays in Monte Carlo simulations, as a means of reducing finite lattice spacing effects, leading to a faster approach to the continuum.

The Wilson fermionic action is a standard implementation of fermions on the lattice. It circumvents the notorious doubling problem by means of a higher derivative term, which removes unphysical propagator poles and has a vanishing classical continuum limit; at the same time, the action is strictly local, which is very advantageous for numerical simulation. The price one pays for strict locality and absence of doublers is, of course, well known: The higher derivative term breaks chiral invariance explicitly. Thus, merely setting the bare fermionic mass to zero is not sufficient to ensure chiral symmetry in the quantum continuum limit; quantum corrections introduce an additive renormalization to the fermionic mass, which must then be fine tuned to have a vanishing renormalized value. Consequently, the hopping parameter  $\kappa$ , which is very simply related to the fermion mass, must be appropriately shifted from its naive value, in order to recover chiral invariance.

By dimensional power counting, the additive mass renormalization is seen to be linearly divergent with the lattice spacing. This adverse feature of Wilson fermions, typical of vacuum expectation values of local objects, poses an additional problem to a perturbative treatment, aside from the usual issues related to lack of Borel summability. Indeed, our calculation serves as a check on the limits of applicability of perturbation theory, by comparison with non perturbative results coming from Monte Carlo simulations.

In the present work we will follow the procedure and notation of Ref. [2], in which  $\kappa_c$  was computed using the Wilson fermionic action without  $\mathcal{O}(a)$  improvement. The results of Ref. [2] were recently confirmed in Ref. [3], in which a coordinate space method was used to achieve even greater accuracy.

The critical fermionic mass and hopping parameter will now depend not only on the number of colors  $N$  and of fermionic flavours  $N_f$ , but also on the free parameter  $c_{\text{SW}}$  which appears in the clover action (see next Section); we will keep this dependence explicit in our results.

In Sec. II we define the quantities which we set out to compute, and describe our calculation. In Sec. III we present our results and compare with Monte Carlo evaluations. Finally, in Sec. IV we obtain improved estimates coming from a tadpole resummation.

## II. FORMULATION OF THE PROBLEM

Our starting point is the Wilson formulation of the QCD action on the lattice, with the addition of the clover (SW) [1] fermion term. Its action reads, in standard notation:

$$S_L = \frac{1}{g_0^2} \sum_{x, \mu, \nu} \text{Tr} [1 - U_{\mu, \nu}(x)] + \sum_f \sum_x (4r + m_B) \bar{\psi}_f(x) \psi_f(x)$$

$$\begin{aligned}
& -\frac{1}{2} \sum_f \sum_{x, \mu} \left[ \bar{\psi}_f(x) (r - \gamma_\mu) U_\mu(x) \psi_f(x + \hat{\mu}) + \bar{\psi}_f(x + \hat{\mu}) (r + \gamma_\mu) U_\mu(x)^\dagger \psi_f(x) \right] \\
& + \frac{i}{4} c_{\text{SW}} \sum_f \sum_{x, \mu, \nu} \bar{\psi}_f(x) \sigma_{\mu\nu} \hat{F}_{\mu\nu}(x) \psi_f(x),
\end{aligned} \tag{1}$$

$$\text{where : } \hat{F}_{\mu\nu} \equiv \frac{1}{8} (Q_{\mu\nu} - Q_{\nu\mu}), \quad Q_{\mu\nu} = U_{\mu, \nu} + U_{\nu, -\mu} + U_{-\mu, -\nu} + U_{-\nu, \mu} \tag{2}$$

Here  $U_{\mu, \nu}(x)$  is the usual product of link variables  $U_\mu(x)$  along the perimeter of a plaquette in the  $\mu$ - $\nu$  directions, originating at  $x$ ;  $g_0$  denotes the bare coupling constant;  $r$  is the Wilson parameter;  $f$  is a flavor index;  $\sigma_{\mu\nu} = (i/2)[\gamma_\mu, \gamma_\nu]$ . Powers of the lattice spacing  $a$  have been omitted and may be directly reinserted by dimensional counting.

The bare fermionic mass  $m_B$  must be set to zero for chiral invariance in the classical continuum limit. The value of the parameter  $c_{\text{SW}}$  can be chosen arbitrarily; it is normally tuned in a way as to minimize  $\mathcal{O}(a)$  effects. Terms proportional to  $r$  in the action, as well as the clover terms, break chiral invariance. They vanish in the classical continuum limit; at the quantum level, they induce nonvanishing, flavor-independent corrections to the fermion masses. Numerical simulation algorithms usually employ the hopping parameter,

$$\kappa \equiv \frac{1}{2m_B a + 8r} \tag{3}$$

as an adjustable quantity. Its critical value, at which chiral symmetry is restored, is thus  $1/8r$  classically, but gets shifted by quantum effects.

The renormalized mass can be calculated in textbook fashion from the fermion self-energy. Denoting by  $\Sigma^L(p, m_B, g_0)$  the truncated, one particle irreducible fermionic two-point function, we have for the fermionic propagator:

$$S(p) = \left[ i \not{p} + m(p) - \Sigma^L(p, m_B, g_0) \right]^{-1} \tag{4}$$

$$\text{where : } \not{p} = \sum_\mu \gamma_\mu \frac{1}{a} \sin(ap^\mu), \quad m(p) = m_B + \frac{2r}{a} \sum_\mu \sin^2(ap^\mu/2).$$

To restore the explicit breaking of chiral invariance, we require that the renormalized mass vanish:

$$S^{-1}(0) = 0 \quad \implies \quad m_B = \Sigma^L(0, m_B, g_0) \tag{5}$$

The above is a recursive equation for  $m_B$ , which can be solved order by order in perturbation theory.

We write the loop expansion of  $\Sigma^L$  as:

$$\Sigma^L(0, m_B, g_0) = g_0^2 \Sigma^{(1)} + g_0^4 \Sigma^{(2)} + \dots \tag{6}$$

Two diagrams contribute to  $\Sigma^{(1)}$ , shown in Fig. I. In these diagrams, the fermion mass must be set to its tree level value,  $m_B \rightarrow 0$ .



FIGURE I. One-loop diagrams contributing to  $\Sigma^L$ . Wavy (solid) lines represent gluons (fermions).

The quantity  $\Sigma^{(2)}$  receives contributions from a total of 26 diagrams, shown in Fig. II. Genuine 2-loop diagrams must again be evaluated at  $m_B \rightarrow 0$ ; in addition, one must include to this order the 1-loop diagram containing an  $\mathcal{O}(g_0^2)$  mass counterterm (diagram 23).

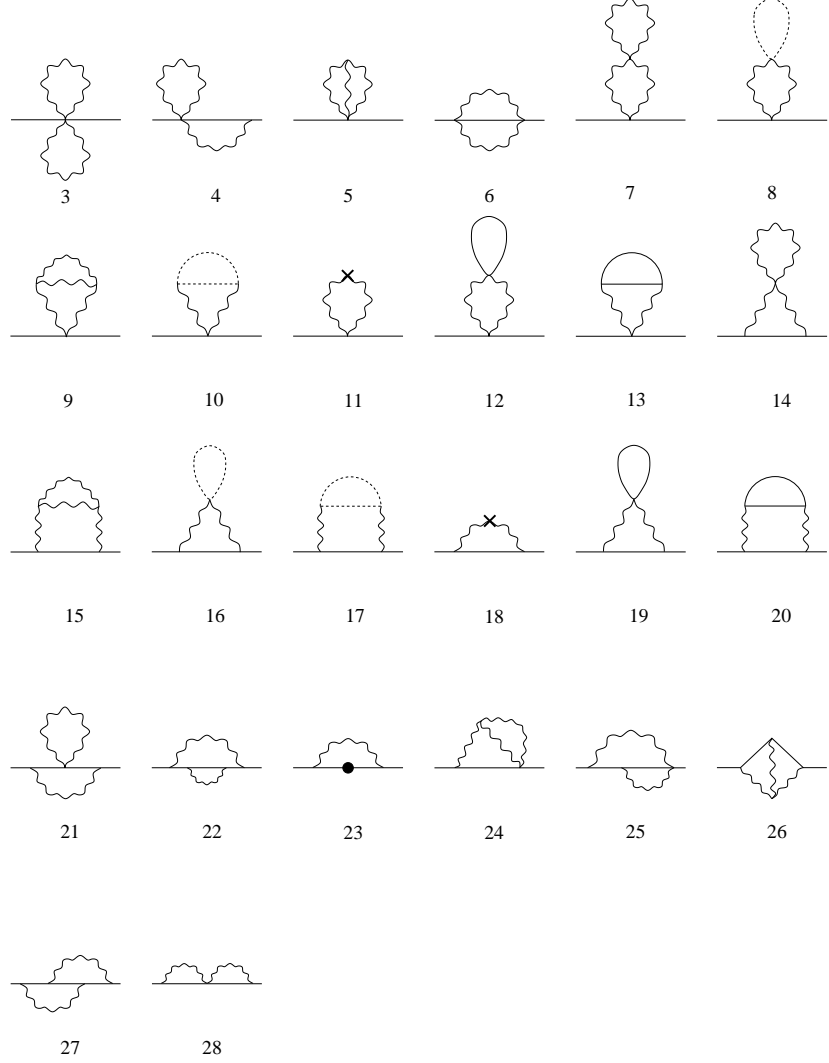


FIGURE II. Two-loop diagrams contributing to  $\Sigma^L$ . Wavy (solid, dotted) lines represent gluons (fermions, ghosts). Crosses denote vertices stemming from the measure part of the action; a solid circle is a fermion mass counterterm.

The contribution of the  $i^{\text{th}}$  diagram can be written in the form

$$(N^2 - 1) \cdot \sum_{j=0}^4 \left( c_{1,i}^{(j)} + \frac{c_{2,i}^{(j)}}{N^2} + \frac{N_f}{N} c_{3,i}^{(j)} \right) c_{\text{SW}}^j \quad (7)$$

where  $c_{1,i}^{(j)}, c_{2,i}^{(j)}, c_{3,i}^{(j)}$  are numerical constants. The dependence on  $c_{\text{SW}}$  is seen to be polynomial of degree 4, as can be verified by inspection of Fig. II.

Certain sets of diagrams, corresponding to renormalization of loop propagators, must be evaluated together in order to obtain an infrared-convergent result: These are diagrams 7+8+9+10+11, 12+13, 14+15+16+17+18, 19+20, 21+22+23.

### III. NUMERICAL RESULTS

Evaluating the two diagrams of Figure I, we find for  $\Sigma^{(1)}$  :

$$\begin{aligned} \Sigma^{(1)} = \frac{N^2 - 1}{N} ( & -0.15493339023106021 & \text{(diagram 1)} \\ & -0.00792366847979(1) + c_{\text{SW}} 0.04348303388205(10) \\ & + c_{\text{SW}}^2 0.01809576878142(1) ) & \text{(diagram 2).} \end{aligned} \quad (8)$$

Here and below we set  $r$  to its usual value,  $r = 1$ . One- and two-loop results pertaining to  $c_{\text{SW}} = 0$  are as in Ref. [2], and can be found with greater accuracy in Ref. [3].

For  $c_{\text{SW}} \neq 0$ , only one-loop results exist so far in the literature; a recent presentation for the case  $c_{\text{SW}}=1$  (see Ref. [4] and earlier references therein) is in perfect agreement with our Eq. (8):

$$\begin{aligned} \Sigma^{(1)}(N=3, c_{\text{SW}}=1) = & -0.2700753495(2) & \text{[Ref. [4]]} \\ & -0.2700753494597(5) & \text{[The present work, Eq. (8)].} \end{aligned} \quad (9)$$

It should be clear to the reader that such a high level of precision is hardly relevant *per se*, especially given the expected deviation from nonperturbative results; nevertheless, it serves as a testing ground for both accuracy and efficiency of our methods, in view of the more demanding higher loop calculations. Further, high precision is called for in the context of the Schrödinger functional computation, to permit a stable extrapolation of various parameters to infinite lattice (see Ref. [4]). Regarding efficiency, let us note that the numerical integrations leading to Eq. (8) require a mere  $\sim 10$  min of CPU time on a typical 1GHz Pentium III processor.

We now turn to the much more cumbersome evaluation of the two-loop diagrams, which is the crux of our present computation. As in Ref. [2], we use a Mathematica package which we have developed for symbolic manipulations in lattice perturbation theory (see, e.g., Ref. [5]). For the purposes of the present work (and a related work on the  $\beta$ -function [6]), we have augmented the package to include the vertices of the clover action.

In Tables I, II, III and IV we present the values of the coefficients  $c_{k,i}^{(1)}, c_{k,i}^{(2)}, c_{k,i}^{(3)}, c_{k,i}^{(4)}$ , respectively. The  $\mathcal{O}(c_{\text{SW}}^0)$  coefficients  $c_{k,i}^{(0)}$  are as in Ref. [2], and have been listed in Table V for completeness. Diagrams giving vanishing contributions to a given power of  $c_{\text{SW}}$  have been omitted from the corresponding table.

The momentum integrations leading to the values of each coefficient are performed numerically on lattices of varying size  $L \leq 32$ , and then extrapolated to infinite lattice size using a broad spectrum of functional forms of the type:  $\sum_{i,j} e_{ij} (\ln L)^j / L^i$ . The systematic

error resulting from the extrapolations has been estimated rather conservatively using the procedure of Ref. [5], and has been included in the tables.

One important consistency check can be performed on those diagrams which are separately IR divergent; taken together in groups, as listed at the end of Section II, they give finite and very stable extrapolations for the coefficients of each power of  $c_{\text{SW}}$ . Several other consistency checks stem from exact relations among various coefficients; to name a few:

$$\begin{aligned} c_{2,4}^{(1)} &= b_2^{(1)} (1/2 - b_1^{(0)}) / 4 \\ c_{2,4}^{(2)} &= b_2^{(2)} / 4 \\ c_{2,7}^{(0)} &= -b_1^{(0)} 3 / 32 \\ c_{2,14}^{(1)} &= -b_2^{(1)} / 8 \\ c_{2,14}^{(2)} &= -b_2^{(2)} / 8 \end{aligned} \quad (10)$$

Here,  $b_i^{(j)}$  are the coefficients of the  $i$ th 1-loop diagram, multiplying  $c_{\text{SW}}^j$ , as displayed in Eq. (8). Comparing with our numerical values of Tables I-IV, we find agreement well within the error bars.

Leaving the choice of values for  $N$ ,  $N_f$  and  $c_{\text{SW}}$  unspecified, our result takes the form:

$$\begin{aligned} \Sigma^{(2)} = (N^2 - 1) [ & (-0.017537(3) & +1/N^2 0.016567(2) & +N_f/N 0.00118618(8)) \\ & + (-0.002601(2) & -1/N^2 0.0005597(7) & -N_f/N 0.0005459(2)) & c_{\text{SW}} \\ & + (-0.0001556(3) & +1/N^2 0.0026226(2) & +N_f/N 0.0013652(1)) & c_{\text{SW}}^2 \\ & + (-0.00016315(6) & +1/N^2 0.00015803(6) & -N_f/N 0.00069225(3)) & c_{\text{SW}}^3 \\ & + (-0.000017219(2) & +1/N^2 0.000042829(3) & -N_f/N 0.000198100(7)) & c_{\text{SW}}^4 \end{aligned} ] \quad (11)$$

To make more direct contact with non-perturbative results, we evaluate  $\Sigma^{(2)}$  at  $N = 3$  and  $N_f = 0, 2$ , obtaining:

$$\begin{aligned} \Sigma^{(2)}(N = 3, N_f = 0) &= -0.12557(3) +0.02031(2) c_{\text{SW}} +0.001087(3) c_{\text{SW}}^2 \\ &\quad -0.001165(1) c_{\text{SW}}^3 -0.00009968(2) c_{\text{SW}}^4 \\ \Sigma^{(2)}(N = 3, N_f = 2) &= -0.11924(3) +0.01740(2) c_{\text{SW}} +0.008368(3) c_{\text{SW}}^2 \\ &\quad -0.004857(1) c_{\text{SW}}^3 -0.0011562(1) c_{\text{SW}}^4 \end{aligned} \quad (12)$$

Eqs. (8, 12) lead immediately to the 1- and 2-loop results for the critical mass:  $m_c^{(1)} = g_0^2 \Sigma^{(1)}$ ,  $m_c^{(2)} = g_0^2 \Sigma^{(1)} + g_0^4 \Sigma^{(2)}$ , and the corresponding hopping parameter  $\kappa_c = 1/(2 m_c a + 8 r)$ .

A number of non-perturbative determinations of  $\kappa_c$  exist in the literature for particular values of  $\beta = 2N/g_0^2$  and  $c_{\text{SW}} \neq 0$ , see e.g. Refs. [7,8] (quenched case) and Refs. [9,10] (unquenched,  $N_f = 2$ ). We present these in Table VI, together with the 1- and 2-loop results ( $\kappa_c^{(1)}$ ,  $\kappa_c^{(2)}$ ). Also included in the Table are the improved results obtained with the method described in the following Section.

#### IV. IMPROVED PERTURBATION THEORY

In order to obtain improved estimates from lattice perturbation theory, one may perform a resummation to all orders of the so-called ‘‘cactus’’ diagrams [11–13]. Briefly stated, these

are gauge-invariant tadpole diagrams which become disconnected if any one of their vertices is removed. The original motivation of this procedure is the well known observation of “tadpole dominance” in lattice perturbation theory. In the following we adapt the calculation of Ref. [2] to the clover action. We refer to Ref. [11] for definitions and analytical results.

Since the contribution of standard tadpole diagrams is not gauge invariant, the class of gauge invariant diagrams we are considering needs further specification. By the Baker-Campbell-Hausdorff (BCH) formula, the product of link variables along the perimeter of a plaquette can be written as

$$\begin{aligned} U_{x,\mu\nu} &= e^{ig_0 A_{x,\mu}} e^{ig_0 A_{x+\mu,\nu}} e^{-ig_0 A_{x+\nu,\mu}} e^{-ig_0 A_{x,\nu}} \\ &= \exp \left\{ ig_0 (A_{x,\mu} + A_{x+\mu,\nu} - A_{x+\nu,\mu} - A_{x,\nu}) + \mathcal{O}(g_0^2) \right\} \\ &= \exp \left\{ ig_0 F_{x,\mu\nu}^{(1)} + ig_0^2 F_{x,\mu\nu}^{(2)} + \mathcal{O}(g_0^4) \right\} \end{aligned} \quad (13)$$

The diagrams that we propose to resum to all orders are the cactus diagrams made of vertices containing  $F_{x,\mu\nu}^{(1)}$ . Terms of this type come from the pure gluon part of the lattice action. These diagrams dress the transverse gluon propagator  $P_A$  leading to an improved propagator  $P_A^{(I)}$ , which is a multiple of the bare transverse one:

$$P_A^{(I)} = \frac{P_A}{1 - w(g_0)}, \quad (14)$$

where the factor  $w(g_0)$  will depend on  $g_0$  and  $N$ , but not on the momentum. The function  $w(g_0)$  can be extracted by an appropriate algebraic equation that has been derived in Ref. [11] and that can be easily solved numerically; for  $SU(3)$ ,  $w(g_0)$  satisfies:

$$u e^{-u/3} \left[ u^2/3 - 4u + 8 \right] = 2g_0^2, \quad u(g_0) \equiv \frac{g_0^2}{4(1 - w(g_0))}. \quad (15)$$

The vertices coming from the gluon part of the action, Eq. (1), get also dressed using a procedure similar to the one leading to Eq. (14) [11]. Vertices coming from the Wilson part of the fermionic action stay unchanged, since their definition contains no plaquettes on which to apply the linear BCH formula; the 3- and 4-point vertices of the clover action, on the other hand, acquire simply a factor of  $(1 - w(g_0))$  [12].

One can apply the resummation of cactus diagrams to the calculation of additive and multiplicative renormalizations of lattice operators. Applied to a number of cases of interest [11,12], this procedure yields remarkable improvements when compared with the available nonperturbative estimates. As regards numerical comparison with other improvement schemes (tadpole improvement, boosted perturbation theory, etc.) [14,15], cactus resummation fares equally well on all the cases studied [13].

One advantageous feature of cactus resummation, in comparison to other schemes of improved perturbation theory, is the possibility of systematically incorporating higher loop diagrams. The present calculation exemplifies this feature, as we will now show.

Dressing the 1-loop results is quite straightforward: the fermionic propagator stays unchanged, the gluon propagator gets multiplied by  $1/(1 - w(g_0))$  and the dressing of the fermionic vertices amounts to a rescaling:  $c_{\text{sw}} \rightarrow c_{\text{sw}} (1 - w(g_0))$ . The resulting values,

$\kappa_{c, \text{dressed}}^{(1)}$ , are shown in Table VI. It is worth noting that these values already fare better than the much more laborious undressed 2-loop results.

We now turn to dressing the 2-loop results. Here, one must take care to avoid double counting: A part of diagrams 4, 7 and 14 has already been included in dressing the 1-loop result, and must be explicitly subtracted from  $\Sigma^{(2)}$  before dressing. Fortunately, this part (we shall denote it by  $\Sigma_{\text{sub}}^{(2)}$ ) is easy to identify, as it necessarily includes all of the  $1/N^2$  part in diagrams 7, 14, and the  $1/N^2$  part of diagram 4 involving a clover 5-point vertex. A simple exercise in contraction of  $SU(N)$  generators shows that  $\Sigma_{\text{sub}}^{(2)}$  is proportional to  $(2N^2 - 3)(N^2 - 1)/(3N^2)$ . There follows without difficulty that:

$$\begin{aligned} \Sigma_{\text{sub}}^{(2)} &= -(2N^2 - 3)(N^2 - 1)/(3N^2) \cdot \\ &[b_2^{(1)} c_{\text{SW}}/8 + c_{2,4}^{(2)} c_{\text{SW}}^2 + c_{2,7}^{(0)} + c_{2,14}^{(0)} + c_{2,14}^{(1)} c_{\text{SW}} + c_{2,14}^{(2)} c_{\text{SW}}^2] \end{aligned} \quad (16)$$

(cf. Eq. (10)).

A potential complication is presented by gluon vertices. While the 3-gluon vertex dresses by a mere factor of  $(1 - w(g_0))$ , the dressed 4-gluon vertex contains a term which is not simply a multiple of its bare counterpart (see Appendix C of Ref. [11]). It is easy to check, however, that this term must simply be dropped, being precisely the one which has already been taken into account in dressing the 1-loop result; the remainder dresses in the same way as the 3-gluon vertex. The very same situation prevails with the dressed 5-point vertex of the clover action, as in diagram 4.

In conclusion, cactus resummation applied to the 2-loop quantity  $\Sigma^{(2)}$  leads to the following rather simple recipe:

$$m_{c, \text{dressed}}^{(2)} = \Sigma^{(1)} \frac{g_0^2}{1 - w(g_0)} + (\Sigma^{(2)} - \Sigma_{\text{sub}}^{(2)}) \frac{g_0^4}{[1 - w(g_0)]^2} \Big|_{c_{\text{SW}} \rightarrow c_{\text{SW}}(1 - w(g_0))} \quad (17)$$

(For the values of  $\beta$  in Table VI,  $\beta = 5.20, 5.26, 5.29, 5.7, 6.0, 6.2, 12.0, 24.0$ , we obtain from Eq. (15):  $1 - w(g_0) = 0.697146, 0.701957, 0.704298, 0.732579, 0.749775, 0.759969, 0.887765, 0.946087$ , respectively.)

Our results for  $\kappa_{c, \text{dressed}}^{(2)}$ , as obtained from Eq. (17), are listed in Table VI. Comparing with the Monte Carlo estimates, dressed results show a definite improvement over non-dressed values. It is interesting to note that 1-loop dressed results already provide most of the improvement, except at very large  $\beta$ -values. At the same time, a sizeable discrepancy still remains, as was expected from start; multiplicative renormalizations, calculated to the same order, are expected to be much closer to their exact values. A first case study of this kind, regarding the  $\beta$ -function with clover improvement, is now complete and will be presented elsewhere [6].

## REFERENCES

- [1] B. Sheikholeslami and R. Wohlert, Nucl. Phys. **B259**, 572 (1985).
- [2] E. Follana and H. Panagopoulos, Phys. Rev. **D63**, 017501 (2001).
- [3] S. Caracciolo, A. Pelissetto, A. Rago, e-print hep-lat/0106013.
- [4] A. Bode, P. Weisz and U. Wolff, Nucl. Phys. **B576**, 517 (2000).
- [5] C. Christou, A. Feo, H. Panagopoulos, and E. Vicari, Nucl. Phys. **B525**, 387 (1998).
- [6] A. Bode and H. Panagopoulos, *The three-loop  $\beta$ -function of QCD with the clover action*, in preparation.
- [7] M. Lüscher, S. Sint, R. Sommer, P. Weisz and U. Wolff, Nucl. Phys. **B491**, 323 (1997).
- [8] UKQCD Collaboration (K.C. Bowler et al.), Phys. Rev. **D62**, 054506 (2000).
- [9] K. Jansen and R. Sommer, Nucl. Phys. **B530**, 185 (1998).
- [10] UKQCD Collaboration (C.R. Allton et al.), e-print hep-lat/0107021.
- [11] H. Panagopoulos and E. Vicari, Phys. Rev. **D58**, 114501 (1998).
- [12] H. Panagopoulos and E. Vicari, Phys. Rev. **D59**, 057503 (1999).
- [13] H. Panagopoulos and E. Vicari, Nucl. Phys. **B (PS) 83**, 884 (2000).
- [14] G. Parisi, in: High-Energy Physics – 1980, XX Int. Conf., Madison (1980), ed. L. Durand and L. G. Pondrom (American Institute of Physics, New York, 1981).
- [15] G. P. Lepage and P. B. Mackenzie, Phys. Rev. **D48**, 2250 (1993).

TABLE I. Coefficients  $c_{1,i}^{(1)}$ ,  $c_{2,i}^{(1)}$ ,  $c_{3,i}^{(1)}$ .  $r = 1$ .

$i$	$c_{1,i}^{(1)}$	$c_{2,i}^{(1)}$	$c_{3,i}^{(1)}$
4	-0.00697298969(1)	0.00711962270(1)	0
12+13	0	0	-0.00005540(1)
14+15+16+17+18	0.005587(1)	-0.0054356(3)	0
19+20	0	0	-0.0004905(2)
21+22+23	0.0015499(6)	-0.0015499(6)	0
24	-0.00022742(6)	0	0
25	0.0014715(3)	-0.00002752(1)	0
26	0.0009439(2)	0	0
27	0	-0.0007525(1)	0
28	0.00024887(3)	0.000086138(5)	0

TABLE II. Coefficients  $c_{1,i}^{(2)}$ ,  $c_{2,i}^{(2)}$ ,  $c_{3,i}^{(2)}$ .  $r = 1$ .

$i$	$c_{1,i}^{(2)}$	$c_{2,i}^{(2)}$	$c_{3,i}^{(2)}$
4	-0.00486917062(1)	0.00452394220(1)	0
6	0.0017538(2)	0	0
12+13	0	0	0.0008949(1)
14+15+16+17+18	0.0021977(2)	-0.0022620(2)	0
19+20	0	0	0.0004703(1)
21+22+23	-0.0001864(1)	0.0001864(1)	0
24	0.00003257(1)	0	0
25	-0.00022829(1)	-0.00005915(1)	0
26	0.00060875(1)	0	0
27	0	0.00035168(2)	0
28	0.00053539(5)	-0.00011818(1)	0

 TABLE III. Coefficients  $c_{1,i}^{(3)}$ ,  $c_{2,i}^{(3)}$ ,  $c_{3,i}^{(3)}$ .  $r = 1$ .

$i$	$c_{1,i}^{(3)}$	$c_{2,i}^{(3)}$	$c_{3,i}^{(3)}$
19+20	0	0	-0.00069225(3)
21+22+23	-0.00017530(6)	0.00017530(6)	0
25	0.000022090(4)	0	0
26	-0.000023954(3)	0	0
27	0	-0.000017264(2)	0
28	0.000014014(3)	0	0

 TABLE IV. Coefficients  $c_{1,i}^{(4)}$ ,  $c_{2,i}^{(4)}$ ,  $c_{3,i}^{(4)}$ .  $r = 1$ .

$i$	$c_{1,i}^{(4)}$	$c_{2,i}^{(4)}$	$c_{3,i}^{(4)}$
19+20	0	0	-0.00019810(1)
21+22+23	-0.000017219(2)	0.000017219(2)	0
27	0	0.000025610(2)	0

TABLE V. Coefficients  $c_{1,i}^{(0)}$ ,  $c_{2,i}^{(0)}$ ,  $c_{3,i}^{(0)}$ .  $r = 1$ .

$i$	$c_{1,i}^{(0)}$	$c_{2,i}^{(0)}$	$c_{3,i}^{(0)}$
3	0.002000362950707492	-0.0030005444260612375	0
4	0.00040921361(1)	-0.00061382041(2)	0
6	-0.0000488891(8)	0.000097778(2)	0
7+8+9+10+11	-0.013927(3)	0.014525(2)	0
12+13	0	0	0.00079263(8)
14+15+16+17+18	-0.005753(1)	0.0058323(7)	0
19+20	0	0	0.000393556(7)
21+22+23	0.000096768(4)	-0.000096768(4)	0
25	0.00007762(1)	-0.00015524(3)	0
26	-0.00040000(5)	0	0
27	0	-0.000006522(1)	0
28	0.0000078482(5)	-0.000015696(1)	0

 TABLE VI. One- and two-loop results  $(\kappa_c^{(1)}, \kappa_c^{(2)})$ , along with their improved (dressed) counterparts, and nonperturbative determinations. See references, shown in square brackets, for details on the nonperturbative definition of  $\kappa$  and on error estimates.

$N_f$	$\beta$	$c_{\text{SW}}$	$\kappa_c^{(1)}$	$\kappa_c^{(2)}$	$\kappa_{c,\text{dressed}}^{(1)}$	$\kappa_{c,\text{dressed}}^{(2)}$	Simulation	
0	5.70	1.568	0.1296	0.1332	0.1366	0.1366	0.1432	[8]
0	6.00	1.479	0.1301	0.1335	0.1362	0.1362	0.1392	[8]
0	6.00	1.769	0.12749	0.13061	0.13372	0.13319	0.13525	[8,7]
0	6.20	1.442	0.1303	0.1334	0.1358	0.1358	0.1379	[8]
0	6.20	1.614	0.12878	0.13182	0.13439	0.13414	0.13582	[8,7]
0	12.0	1.1637	0.128766	0.129622	0.129807	0.129845	0.129909	[7]
0	24.0	1.0730	0.127019	0.127229	0.127243	0.127253	0.127258	[7]
2	5.20	2.0171	0.12515	0.12987	0.13481	0.13342	0.13663	[10,9]
2	2.26	1.9497	0.12589	0.13043	0.13517	0.13392	0.13709	[10,9]
2	2.29	1.9192	0.12622	0.13068	0.13532	0.13414	0.13730	[10,9]